
Physiologically based modeling of the effect of physiological and anthropometric variability on indocyanine green based liver function tests

Adrian Köller¹, Jan Grzegorzewski¹ and Matthias König^{1,*}

¹ Institute for Theoretical Biology, Institute of Biology, Humboldt University, Berlin, Germany

Correspondence*:

Matthias König
koenigmx@hu-berlin.de

2 ABSTRACT

Accurate evaluation of liver function is a central task in hepatology. Dynamic liver function tests (DLFT) based on the time-dependent elimination of a test substance provide an important tool for such a functional assessment. These tests are used in the diagnosis and monitoring of liver disease as well as in the planning of hepatobiliary surgery. A key challenge in the evaluation of liver function with DLFTs is the large inter-individual variability. Indocyanine green (ICG) is a widely applied test compound used for the evaluation of liver function. After an intravenous administration, pharmacokinetic (PK) parameters are calculated from the plasma disappearance curve of ICG which provide an estimate of liver function. The hepatic elimination of ICG is affected by physiological factors such as hepatic blood flow or binding of ICG to plasma proteins, anthropometric factors such as body weight, age, and sex, or the protein amount of the organic anion-transporting polypeptide 1B3 (OATP1B3) mediating the hepatic uptake of ICG. Being able to account for and better understand these various sources of inter-individual variability would allow to improve the power of ICG based DLFTs and move towards an individualized evaluation of liver function. Within this work we systematically analyzed the effect of various factors on ICG elimination by the means of computational modeling. For the analysis, a recently developed and validated physiologically based pharmacokinetics (PBPK) model of ICG distribution and hepatic elimination was utilized. Key results are (i) a systematic analysis of the variability in ICG elimination due to hepatic blood flow, cardiac output, OATP1B3 abundance, liver volume, body weight and plasma bilirubin level; (ii) the evaluation of the inter-individual variability in ICG elimination via a large *in silico* cohort of n=100000 subjects based on the NHANES cohort with special focus on stratification by age, sex, and body weight; (iii) the evaluation of the effect of various degrees of cirrhosis on variability in ICG elimination. The presented results are an important step towards individualizing liver function tests by elucidating the effects of confounding physiological and anthropometric parameters in the evaluation of liver function via ICG.

Keywords: Indocyanine Green, ICG, Liver Cirrhosis, Mathematical Model, Computational Model, Pharmacokinetics, Liver Function, PBPK

1 INTRODUCTION

29 Accurate evaluation of liver function is a central task in hepatology. Dynamic liver function tests (DLFT)
30 based on time-dependent elimination of test substances provide an important tool for the functional
31 assessment of the liver. These tests are used in the diagnosis and monitoring of liver disease as well as in
32 the planning of hepatobiliary surgery.

33 Indocyanine green (ICG) is a widely applied test compound used for the evaluation of liver function. It
34 is bound to plasma proteins in the blood, eliminated exclusively by the liver, and subsequently excreted
35 into the bile. It is not reabsorbed by the intestinal tissue and therefore does not undergo enterohepatic
36 circulation (Wheeler et al., 1958). After intravenous administration of ICG, the plasma disappearance
37 curve of ICG can be measured either by repeated plasma sampling or through non-invasive fingertip
38 methods. From the concentration-time profile a set of pharmacokinetic parameters can be calculated
39 (e.g. ICG clearance, plasma disappearance rate (ICG-PDR), retention ratio after 15 minutes (ICG-R15),
40 ICG half-life), which provide estimates of liver function based on the ICG elimination capacity of the
41 liver (Köller et al., 2021; Sakka, 2018).

42 A major challenge in DLFTs based on the elimination of test substances such as ICG is the large inter-
43 individual variability in their elimination. Physiological factors such as hepatic blood flow, binding to
44 plasma proteins, or the amount of transport protein mediating the hepatic ICG uptake can influence the
45 elimination of ICG. Furthermore, ICG elimination is generally reduced in liver disease and altered by
46 surgical interventions such as partial hepatectomy (Köller et al., 2021).

47 1.1 Blood flow

48 The elimination of ICG depends strongly on hepatic blood flow due to its high hepatic extraction-ratio
49 (0.6 - 0.9 in healthy subjects (Grainger et al., 1983)). The effect of varying hepatic blood flow on ICG-
50 elimination has been studied by various groups. Kanstrup and Winkler found a strong positive correlation
51 between hepatic blood flow and ICG-clearance when altering hepatic blood flow either pharmacologically
52 or by food ingestion (Kanstrup and Winkler, 1987). Rowell et al. reported a strong positive correlation
53 between changes in hepatic blood flow and ICG-clearance during exercise in healthy subjects but poor
54 correlation in cirrhosis (Rowell et al., 1964). Gadano et al. and Huet and Villeneuve studied the dependency
55 of ICG-clearance on hepatic blood flow in cirrhotic and healthy subjects (Gadano et al., 1997; Huet and
56 Villeneuve, 1983). Huet and Lelorier were interested in the effects of smoking and chronic hepatitis B
57 reporting hepatic blood flow and ICG parameters (Huet and Lelorier, 1980).

58 Hepatic blood flow results from the interplay of various factors such as blood pressure, portal resistance
59 and cardiac output. Further, it is often altered in disease (e.g. in portal hypertension (Iwakiri, 2014)) and
60 after liver surgery (e.g. partial hepatectomy (Kawasaki et al., 1991)). As a consequence, accurate evaluation
61 of liver function via ICG pharmacokinetics is challenging in diseases that affect systemic circulation
62 (e.g. cardiac output) or hepatic blood supply. A better understanding of the effects of blood flow on ICG
63 elimination would enable a more accurate evaluation of ICG liver function tests.

64 1.2 Transport protein (OATP1B3)

65 ICG is removed from the blood via transporter-mediated uptake into the hepatocytes. Two proteins on
66 the sinusoidal membrane are mainly responsible for the hepatic uptake of ICG in humans, the organic
67 anion transporting polypeptide 1B3 (OATP1B3, gene symbol: SLCO1B3) and the Na⁺-taurocholate
68 cotransporting polypeptide (NTCP) (de Graaf et al., 2011; Kagawa et al., 2017). OATP1B3 is the major
69 transporter for hepatic ICG uptake and subjects with a homozygous SLCO1B3 null allele show markedly
70 impaired ICG clearance (Anzai et al., 2020).

71 The OATP level in hepatocytes has a large impact on plasma concentrations of various drugs (Giacomini
72 et al., 2010; Schipani et al., 2012; Schneck et al., 2004). In human subjects, a large variability in the protein
73 amount of OATP1B3 exists (Burt et al., 2016; Kimoto et al., 2012; Prasad et al., 2014). The OATP1B3
74 level does not depend on age or sex (Prasad et al., 2014) though some dependency on ethnicity has been
75 reported (Peng et al., 2015).

76 1.3 Plasma proteins and bilirubin

77 ICG is bound to plasma proteins (serum albumin and lipoproteins) (Kamisaka et al., 1974; Ott, 1998). It
78 has been suggested that these plasma proteins are involved in the hepatic uptake mechanism of ICG at the
79 sinusoidal membrane (Berk et al., 1987; Shinohara et al., 1996). However, no consensus about the effect of
80 plasma proteins on ICG uptake has been reached. In contrast, the effect of bilirubin on ICG uptake has been
81 extensively studied. Bilirubin is an end product of heme degradation which is primarily located in the blood
82 and is almost completely bound to albumin (Fevery, 2008; Maruhashi et al., 2019). Significant negative
83 correlation between ICG elimination and plasma bilirubin levels has been reported (Branch et al., 1976;
84 Paumgartner et al., 1969). Changes in bilirubin plasma levels are often induced by hepato-biliary diseases,
85 with the prime example being Gilbert's disease (Fretzayas et al., 2012). Further, increased bilirubin plasma
86 levels can be caused by biliary obstruction or viral hepatitis and are used as an indicator of acute liver
87 failure (Sullivan and Rockey, 2017).

88 1.4 Anthropometric factors

89 An important question for the individualized and stratified evaluation via DLFTs is how factors such
90 as body weight, age, and sex affect the elimination of the test substance. As summarized by Kim et
91 al. (Kim et al., 2015), age has a significant effect on liver volume, blood flow, and function. A reduction
92 of functional liver mass, total liver volume, and a decrease in hepatic blood flow are the most relevant
93 age induced changes to the liver. Additionally, the susceptibility to liver disease increases with age
94 accompanied by a decline in the hepatic regenerative response which has substantial consequences for
95 liver surgery (Schmucker, 2005). Reduced ICG clearance with increasing age has been reported by Wood
96 et al. (Wood et al., 1979). Liver volume and body weight have been shown to correlate well in western
97 adults (Vauthey et al., 2002). Due to the dependency of ICG elimination on liver volume (Roberts et al.,
98 1976), body weight is an important factor to be considered in the evaluation of liver function with ICG.
99 Because of significant differences in average body weight and organ volumes between male and female
100 subjects, sex is another important factor in the analysis of variability in ICG liver function tests. However,
101 Martin et al. (Martin et al., 1975) reported no variations in ICG-clearance per kg body weight between
102 male and female subjects, while reporting significantly increased ICG-PDR in women.

103 Within this work we systematically investigated the individual contribution of these factors to the large
104 inter-individual variability in liver function tests based on ICG using a recently developed and validated
105 physiologically based pharmacokinetics (PBPK) model of ICG (Köller et al., 2021).

2 MATERIAL AND METHODS

106 The presented work utilizes a recently established and validated PBPK model of ICG distribution
107 and hepatic elimination (Fig. 1). The model is encoded in the Systems Biology Markup Language
108 (SBML) (Hucka et al., 2019; Keating et al., 2020) and was developed using sbmlutils (König, 2021b),
109 and cy3sbml (König and Rodriguez, 2019). Simulations were performed using sbmlsim (König, 2021a)
110 based on the high-performance SBML simulator libroadrunner (Somogyi et al., 2015). We refer to (Köller
111 et al., 2021) for details on the computational model, the model simulations, the data curation process, the

112 calculation of pharmacokinetic parameters, and the implementation of liver cirrhosis. No model changes
113 were performed compared to the model described in (Köller et al., 2021).

114 2.1 Parameter scans

115 Parameter scans (Fig. 2) were performed by varying the model parameters corresponding to the relative
116 change in hepatic blood flow $f_{bloodflow}$ [-], relative change in cardiac output $f_{cardiac_output}$ [-], relative
117 change in OATP1B3 amount $f_{oatp1b3}$, liver volume $FVli$ [l/kg], body weight BW [kg], and plasma
118 bilirubin concentration $bilext$ [-]. The parameter values of the unchanged model are indicated as reference
119 in the plots. For the relative changes $f_{bloodflow}$, $f_{cardiac_output}$, and $f_{oatp1b3}$ the reference parameter value
120 is 1.0 [-]. Bilirubin scans were performed on a log scale whereas all other scans were performed on a linear
121 scale.

122 2.2 In silico population

123 For the analysis of variability in ICG pharmacokinetics, a large dataset of *in silico* individuals was
124 created (see Fig. 5). Age, body weight, sex, height, and ethnicity were based on subjects sampled from the
125 National Health and Nutrition Examination Survey (NHANES) spanning the years 1999-2018 (NHANES,
126 1999-2018). Due to the sampling from a real cohort it was possible to account for the covariances between
127 the respective variables. Children and adolescents (age < 18 years), obese subjects ($BMI > 30$), and
128 subjects with age ≥ 85 from 1999-2006 and ≥ 80 from 2007-2018 (due to top coding in NHANES at
129 85 and 80 years, respectively) were excluded. The resulting 35427 subjects were oversampled to reach
130 100000 individuals. This ensured sufficient samples in all stratified subgroups. Based on the age of a
131 given individual, liver volume and hepatic blood flow were determined by multivariate sampling of liver
132 volume per body weight and hepatic blood flow per body weight from the respective age distribution and
133 subsequent multiplication with the individual body weight. This allowed to account for the covariances
134 between liver volume and blood flow as well as the dependency of age. The normal distributions and
135 covariance-matrices used for the sampling were calculated from data from Wynne et al. (Wynne et al.,
136 1989). The transport protein amount (OATP1B3) was sampled independently from a lognormal distribution
137 that was fitted to data from Peng et al. (Peng et al., 2015). The OATP1B3 distribution was assumed age
138 and sex independent as reported by Prasad et al. (Prasad et al., 2014). Individual model simulations were
139 performed by adjusting the model parameters corresponding to individual body weight BW [kg], liver
140 volume $FVli$ [l/kg], hepatic blood flow $f_{bloodflow}$ [-], and amount of OATP1B3 $f_{oatp1b3}$ [-]. The scaling
141 factors $f_{bloodflow}$ and $f_{oatp1b3}$ describe the relative change from the model reference state. Individual ICG
142 liver function test simulations were performed by administering 0.5 [mg/kg] ICG to the respective virtual
143 individual and calculating the pharmacokinetics parameters on the resulting time course.

3 RESULTS

144 Within this work we systematically analyzed the effect of various factors on ICG elimination by the means
145 of computational modeling. For the analysis, a recently developed and validated PBPK model of ICG
146 distribution and hepatic elimination (see Fig. 1) was utilized (Köller et al., 2021). Model predictions were
147 validated with data from multiple publications with an overview over all data sets provided in Tab. 1.

148 3.1 PBPK Model

149 The systemic blood flow of the PBPK model is based on the cardiac output, which is scaled by the body
150 weight. The liver is perfused through a dual blood supply consisting of arterial blood from the hepatic
151 artery and venous blood from the portal vein. All organs besides the liver, the gastrointestinal tract, and the
152 lung were pooled into the rest compartment. The included hepatic metabolism and biliary excretion are
153 depicted in Fig. 1B. ICG is imported in the liver via OATP1B3. Hepatic ICG is exported through the bile

and subsequently excreted via the feces. The effect of bilirubin on hepatic ICG uptake was modeled as a competitive inhibition based on the assumption that ICG can only be eliminated from the plasma if bound to plasma proteins. Due to the sequestration of plasma proteins bilirubin acts as a competitive inhibitor of ICG elimination, as both substances compete for plasma protein binding sites. Plasma bilirubin levels change slowly compared to the timescale of ICG liver function tests (15 min) and were therefore assumed in steady-state. Liver cirrhosis was modeled by a combination of functional tissue loss and shunts. For a detailed description of the model we refer to (Köller et al., 2021).

3.2 Variability due to physiological factors

First a systematic analysis of the effect of physiological variation on ICG parameters was performed (see Fig. 2). Specifically, the dependency of ICG-clearance, ICG-PDR, ICG-R15 and ICG-t_{1/2} on hepatic blood flow, cardiac output, transport protein amount (OATP1B3), liver volume, body weight, and plasma bilirubin was analyzed. An increase in all physiological factors except the plasma bilirubin concentration results in an increase in ICG elimination (increased ICG-PDR and ICG-clearance, reduced ICG-R15 and ICG-thalf). Changes in blood flow, OATP1B3 level, and liver volume have similar nonlinear effects on ICG parameters, whereas the body weight has an almost linear effect on ICG-clearance but only minimal effects on the other parameters. In the model, liver volume (tissue and blood vessels) are scaled with the body weight. As a result the plasma volume which is cleared from ICG every minute (clearance) increases with the body weight, without any change to the plasma disappearance rate, retention ratio or half-life.

Mild, moderate and severe cirrhosis reduce ICG elimination (decreased ICG-clearance and ICG-PDR, increased ICG-R15 and ICG-thalf) in a step-wise fashion without changing the overall curve shapes.

3.3 Validation of physiological factors

Model predictions were validated using various clinical data sets from healthy controls and subjects with mild, moderate and severe cirrhosis corresponding to Child-Turcotte-Pugh (CTP) classes A, B, and C, respectively (see Fig. 2: ICG-clearance, ICG-PDR, ICG-R15, and ICG-thalf depending on hepatic blood flow (Grundmann et al., 1992; Møller et al., 1998, 2019; Pind et al., 2016; Skak and Keiding, 1987); ICG-clearance, ICG-R15 and ICG-t_{1/2} depending on cardiac output (Grundmann et al., 1992; Pind et al., 2016); ICG-PDR and ICG-R15 depending on OATP1B3 (Anzai et al., 2020; Kagawa et al., 2017; Namihisa et al., 1981); ICG-clearance, ICG-PDR, and ICG-R15 depending on liver volume (Haimerl et al., 2016; Hashimoto and Watanabe, 2000; Roberts et al., 1976); ICG-clearance and ICG-PDR depending on body weight (Haimerl et al., 2016; Huet and Villeneuve, 1983). The model predictions show very good agreement with the validation data.

Additional validation of the model predictions were performed for the dependency of ICG parameters on blood flow (see Fig. 3) and plasma bilirubin (see Fig. 4).

Fig. 3A and B show the relation between ICG-clearance and hepatic blood flow in healthy subjects as well as patients of chronic hepatitis B or C and liver cirrhosis. ICG-clearance is reduced in liver disease, more severely in liver cirrhosis than hepatitis. The simulations were performed for healthy controls and three different degrees of cirrhosis (mild, moderate, severe) and are in good agreement with the clinical data (Gadano et al., 1997; Huet and Lelorier, 1980; Huet and Villeneuve, 1983). Subjects with hepatitis compare well to the simulation of moderate cirrhosis. Fig. 3C shows the change in ICG-clearance due to an externally induced change in hepatic blood flow by exercise, food ingestion or pharmacological intervention (Kanstrup and Winkler, 1987) with the corresponding model simulation. The relation is predicted accurately by the model, with an increase in blood flow resulting in an increased clearance of ICG. In Fig. 3D the dependency of the ICG extraction ratio on the hepatic blood flow is depicted. The

197 extraction-ratio is the fraction of drug, that is removed from the plasma after a single pass through the liver.
198 With increasing hepatic blood flow the extraction ratio decreases with model predictions for healthy and
199 cirrhotic subjects being in good agreement with the data (Leevy et al., 1962).

200 The bilirubin plasma concentration in healthy subjects shows little variation (Fig. 4A-C, E, F). However,
201 in liver cirrhosis and other liver diseases bilirubin levels may vary by an order of magnitude and are
202 generally increased. The simulations depicted in Fig. 4 were performed for healthy controls and three
203 different cirrhosis degrees based on the assumption of competitive inhibition of ICG uptake by bilirubin.
204 Results were compared to clinical data of control and diseased subjects. Fig. 4 shows the dependency
205 of ICG parameters on the plasma bilirubin levels (A, B: ICG-clearance; C: ICG-kel; D: ICG-R15; E:
206 ICG-R20; F: ICG extraction ratio). Overall the decrease in ICG elimination due to elevated bilirubin plasma
207 levels is predicted accurately. The simulations for healthy controls agree well with the data in healthy
208 subjects.

209 In summary, model predictions for the effect of hepatic blood flow, cardiac output, OATP1B3 level, liver
210 volume, body weight and bilirubin on ICG parameters could be validated with a large set of studies in
211 healthy controls and various degrees of cirrhosis spanning almost 60 years of clinical research (Anzai et al.,
212 2020; Branch et al., 1976; Caesar et al., 1961; D’Onofrio et al., 2014; Gadano et al., 1997; Grundmann
213 et al., 1992; Haimerl et al., 2016; Hashimoto and Watanabe, 2000; Huet and Lelorier, 1980; Huet and
214 Villeneuve, 1983; Kagawa et al., 2017; Kanstrup and Winkler, 1987; Kawasaki et al., 1988; Leevy et al.,
215 1962, 1967; Møller et al., 1998, 2019; Namihsa et al., 1981; Pind et al., 2016; Roberts et al., 1976; Skak
216 and Keiding, 1987).

217 **3.4 *In silico* population**

218 To analyze the inter-individual variability of ICG parameters, *in silico* ICG liver function tests were
219 performed for 100000 subjects (Fig. 5. For every individual the age, body weight, sex, height and ethnicity
220 was based on the NHANES cohort with subsequent sampling of age-dependent liver volume and hepatic
221 blood flow and OATP1B3 amount. The 35427 NHANES subjects were oversampled to 100000 subjects,
222 i.e., every subject occurred around three times with different liver volume and hepatic blood flow samples.
223 By sampling from a large cohort of real individuals the covariances between the parameters age, body
224 weight, sex, height and ethnicity could be accounted for. *In silico* ICG liver function tests used a dose
225 of 0.5 [mg/kg] ICG (Fig. 5A). The dependency of the body weight on the age in men and women in the
226 simulated population are depicted in Fig. 5B and C, respectively. In general, women have a lower body
227 weight. Both distributions show an increase in body weight up until 40-60 year, followed by a decline in
228 older ages. The number of subjects in younger age-groups is higher than in older age-groups, although this
229 might not be representative of the population, but rather of the NHANES study design.

230 For every virtual individual the OATP1B3 level was sampled from a lognormal distribution based on
231 reported protein concentrations by Peng et al. (Peng et al., 2015) (see Fig. 5D). OATP1B3 samples were
232 assumed to be independent of age, body weight, sex, height and ethnicity.

233 For every virtual individual the age-dependent liver volume and hepatic blood flow were sampled under
234 consideration of the underlying covariances between hepatic blood flow per kg body weight and liver
235 volume per kg body weight, based on data by Wynne et al. (Wynne et al., 1989) (Fig. 5E-G). Both liver
236 volume and hepatic blood flow per body weight decrease with increasing age. Age dependent multivariate
237 sampling was used to determine hepatic blood flow and liver volume for every virtual individual, i.e.
238 samples were taken from the respective age-dependent distribution.

239 3.5 Inter-individual variability

240 The inter-individual variability in ICG elimination was analyzed by performing an individualized ICG
241 test simulation for each of the n=100000 subjects. ICG parameters were calculated from the individual ICG
242 time courses. To analyse the effect of age, body weight and sex on ICG elimination the population was
243 stratified by age (18-40 yr, 41-65 yr, 66-84 yr), body weight (40-60 kg, 60-80 kg, 80-100 kg, 100-140 kg),
244 and sex (M, F). ICG clearance, PDR, R15, and $t_{1/2}$ for each subgroup are shown in Fig. 6. With increasing
245 age (independent of body weight), ICG elimination is reduced, as reflected by a decrease in clearance and
246 PDR and an increase in ICG-R15 and $t_{1/2}$. With increasing body weight ICG clearance increases whereas
247 PDR, R15 and $t_{1/2}$ show no change. Variation in body weight has a much larger effect on ICG-clearance,
248 than on any other PK parameter in line with Fig. 2E.

249 Differences between the sexes are marginal in all parameters after stratification for body weight and age.
250 Due to the lower body weight of women as depicted in Fig. 5B and C and the body weight dependency
251 of ICG clearance an apparent difference between male and female ICG-clearance can be observed in the
252 unstratified data.

253 The corresponding dependencies in mild cirrhosis, moderate cirrhosis, and severe cirrhosis are depicted
254 in Supplementary Fig. 1, 2, and 3, respectively. Similar to healthy subjects, ICG elimination is reduced in
255 cirrhosis with increasing age, as reflected by a decrease in clearance and PDR and an increase in ICG-R15
256 and $t_{1/2}$. With increasing cirrhosis degree ICG clearance and PDR decrease and R15 and $t_{1/2}$ increase, in
257 line with Fig. 2.

258 3.6 Validation of population variability

259 To validate the results of the population model predictions (Fig. 6) multiple comparisons to clinical data
260 sets were performed (Fig. 7 and Fig. 8).

261 The predicted dependency of ICG-clearance and ICG-kel on age in the *in silico* population in Fig. 7 is in
262 very good agreement with data for healthy controls (Branch et al., 1976; Caesar et al., 1961; Kawasaki et al.,
263 1988; Wood et al., 1979), and cirrhosis (Branch et al., 1976; Caesar et al., 1961; Jost et al., 1987; Kawasaki
264 et al., 1988). ICG-clearance and ICG-kel decrease with increasing age and with increasing cirrhosis degree.
265 The clinical data for cirrhosis did not provide any information on the disease severity such as CTP scores,
266 so that cirrhosis data is plotted for all simulated severities. The model predictions cover the complete range
267 of reported ICG-clearance and ICG-kel in cirrhotic subjects.

268 For additional validation, the population variability in the dependency of ICG parameters on hepatic
269 blood flow was studied in Fig. 8A-D) (corresponding to Fig. 3).

270 Fig. 8A and B show the effect of inter-individual differences on the dependency of ICG-clearance on
271 hepatic blood flow. The resulting variability especially in the control samples (grey area), is very large
272 emphasizing the importance of including confounding factors in the evaluation of liver function.

273 Fig. 8C shows the change in ICG-clearance when hepatic blood flow is changed either by exercise,
274 food ingestion or by pharmacological intervention. By including the inter-individual differences in the
275 simulation, we were able to predict the variability in this dependency accurately. From the clinical data, we
276 assume however, that the external influences, that were used to alter hepatic blood flow, had additional
277 effects on ICG elimination, because even subjects with unchanged hepatic blood flow showed a decrease
278 in clearance. It would be of high interest to analyze what these effects might be. This also shows, that
279 recent food ingestion and long-term medication that affects blood flow are additional factors that have to
280 be considered in liver function evaluation with ICG.

Fig. 8D shows the relation between the ICG extraction ratio and the hepatic blood flow. The changes in extraction ratio are in good agreement with the clinical data, but the simulations taking inter-individual into account cover a much larger range of blood flow per body surface area than the data.

Next, the inter-individual variability in the correlations between ICG parameters in healthy and cirrhotic subjects were simulated (Fig. 8E-H). The corresponding results without variability have been published previously (Köller et al., 2021).

Interestingly, all variability in the correlation between ICG-R20 and ICG-t_{1/2} as well as ICG-R20 and ICG-kel lies on a nonlinear relationship (see Fig. 8E and F). Moreover, the clinical data follows the same nonlinear dependencies. Because all PK parameters of a subject are calculated from the same plasma disappearance curve, the results follow a strict nonlinear relationship.

In Fig. 8G the correlation between ICG-PDR after ICG doses of 0.5 mg/kg and 5.0 mg/kg is depicted. The relation is mostly linear, however some variation is observed, which agrees very well with the clinical data. This suggests a small dose-dependency of ICG-PDR depending on individual subject properties. In a previous analysis we could not find any dose-dependency of ICG-PDR for the model with reference parameters (Köller et al., 2021). A more detailed investigation into the factors causing the PDR dose dependency would be highly relevant.

A linear correlation, without deviation due to inter-individual differences, is observed between ICG-clearance calculated after a bolus administration and during a constant intravenous infusion of ICG (see Fig. 8H) with the clinical data following the same linear dependency.

3.7 Contribution of individual factors

Finally, we were interested in the contribution of individual factors to the observed population variability (Fig. 9 using a data set of ICG-clearance and ICG-PDR by Sakka and van Hout (Sakka and van Hout, 2006). The predicted variability between ICG-clearance and ICG-PDR in the *in silico* population is in very good agreement with the observed variability in the data (Fig. 9A). The combined effect of variation in hepatic blood flow, OATP1B3 amount, liver volume and body weight predicts the variability in the clinical data very accurately.

To study the individual contribution of each of the above-mentioned factors these factors were varied individually while setting the remaining factors to their reference values (Fig. 9B-E). Hepatic blood flow, OATP1B3 amount, and liver volume affect ICG-clearance and PDR in a similar manner resulting in a linear dependency. Compared to the model's reference simulation, these factors are able to increase as well as reduce ICG elimination. The individual effects appear to be additive as none of them individually can achieve the complete range of variability that is observed when they are varied together (Fig. 9A). In contrast, the body weight has a much smaller effect on ICG-PDR than on ICG-clearance thereby spanning an alternative axis of variation. Specifically, it is the main source of deviation from the correlation line between PDR and clearance.

4 DISCUSSION

Within this work, the effects of physiological and anthropometric factors on ICG elimination were studied systematically. For the analysis, a recently developed and validated PBPK model of ICG (see Fig. 1) was used (Köller et al., 2021).

The previous modeling approach was extended by the development of a large *in silico* population based on the NHANES cohort (NHANES, 1999-2018) with individualized model predictions for the n=100000 subjects. Our approach allowed to account for covariances between age, sex, body weight, height and

ethnicity as well as age, liver volume and hepatic blood flow. Via individualized *in silico* ICG liver function tests, the inter-individual variability in ICG-elimination could be studied in healthy subjects as well as in mild, moderate, and severe cirrhosis corresponding to CTP-A, CTP-B, and CTP-C. Model predictions were validated with independent clinical data sets from 25 publications which were not used in the model development (see Tab. 1 and figures). Including the variability of physiological factors (hepatic blood flow, cardiac output, OATP1B3 level, liver volume, plasma bilirubin) and anthropometric parameters (body weight, age, sex) in the model simulations allowed to accurately predict the individual effects of these factors as well as the observed inter-individual variability in ICG elimination. The importance of including these factors in the evaluation of liver function with ICG is apparent.

Certain limitations exist in the presented analysis. First, the analysis focused specifically on factors for which (i) clinical data is available, (ii) alterations in ICG elimination are expected, (iii) and which could be included in our PBPK modeling approach. This analysis is far from exhaustive and other factors may exist which influence ICG-elimination but were not considered here. Second, the distributions of liver volume, hepatic blood flow and OATP1B3 amount were based on clinical data with relatively small sample size. The resulting distributions do not necessarily reflect the distribution and covariances within the NHANES population. For instance, some ethnical differences in OATP1B3 distribution may exist that were not considered here (see below for details). Furthermore, parameters which were assumed statistically independent could actually have dependencies. For example, an important assumption was that the amount of OATP1B3 is independent of other sampled factors such as body weight, age, sex, liver volume, and liver blood flow. Prasad et al. showed that OATP1B3 is independent of age and sex (Prasad et al., 2014), yet no data for the relationship between OATP1B3 amount and other anthropometric factors (body weight, liver volume, and liver blood flow) could be found in the literature.

A key factor for ICG elimination is the amount of OATP1B3 in the liver as it is the primary transport protein mediating hepatic ICG uptake. An increase in its amount results in increased ICG elimination (Fig-2C). A previous study has shown that ICG uptake into the liver correlates with the expression of OATP1B3 (Masuoka et al., 2020). Whereas some studies quantified the OATP1B3 amount in Human liver samples (Burt et al., 2016; Peng et al., 2015; Prasad et al., 2014) to our knowledge no data reporting OATP1B3 amount and systemic ICG parameters exists. For validation we compared reported ICG-PDR and ICG-R15 values for different genotypes. Under the assumed transport activities (wildtype enzyme 1.0, heterozygote null genotype 0.5, homozygote null genotype 0.0) for the model predictions, the simulations and experimental data are in very good agreement. Although OATP1B3 expression were significantly lower in the heterozygote than in the wild-type, the ICG-R15 results were comparable (Anzai et al., 2020), suggesting that some compensation is possible. Subjects with markedly poor ICG clearance but without severe liver disease are diagnosed with constitutional ICG excretory defect (Anzai et al., 2020; Namihisa et al., 1981) and lack of OATP1B3 expression has been confirmed in these subjects by immunohistochemistry (Kagawa et al., 2017; Masuoka et al., 2020). The incidence of ICG excretory defect is 0.007% in the Japanese population (Masuoka et al., 2020). Anzai et al. emphasized the importance of investigating the effect of the SLCO1B3 genotype on ICG clearance in cirrhotic patients in the future (Anzai et al., 2020). Within this work, this important investigation could be performed *in silico* (Fig. 2).

Whereas no differences in OATP1B3 expression with age or sex have been reported (Prasad et al., 2014), a difference in OATP1B3 amount with ethnicity may exist. Peng et al. showed based on a relatively small study ($n=102$ Caucasian, $n=18$ Asian, $n=5$ African-American) (Peng et al., 2015) that Asians have almost double the OATP1B3 amount with 27.6 [fmol/ μ g] (24.5 - 30.7 95% CI) of Caucasians with only 14.2 [fmol/ μ g] (12.9 - 15.6 95% CI). Ethnicity information was available for all our *in silico* subjects,

but unfortunately not compatible with the ethnicity groups provided by Peng et al. E.g. Asians were not separately listed in NHANES but part of the larger group 'Other Race - Including Multi-Racial'. In summary, the available information on the ethnicity dependency of OATP1B3 expression was not sufficient to include it in our simulations.

The influence of hepatic blood flow on ICG-elimination was analyzed extensively (see Fig. 2A and B; Fig. 3; Fig. 8E-F). As can be observed in Fig 2A and B, the model's reference values for cardiac output and hepatic blood flow consistently lie below the mean values from clinical data at the lower end of the physiological range. Using relatively low cardiac output in the reference state was necessary to accurately predict the ICG extraction ratio without implementing a longer delay between blood exiting the liver and entering the liver again (which would either require delayed differential equations or constructs such as the linear chain trick to achieve sufficient delays). This simplification had no effect on the ICG plasma disappearance curve and the resulting PK parameters. However, as a side effect of this, the hepatic blood flow of the reference simulations (stars) depicted in Fig. 8A, B and D are at the lower ends of the simulated range. This has no relevance for the variability analysis, but moving towards individualized ICG liver function tests the implementation of a circulation delay will be necessary.

In spite of the observed relationship between the plasma bilirubin concentration and ICG-elimination (see Fig. 2F and 4), it was not included in the population variability analysis. The main reason for this is the low variability of plasma bilirubin in healthy subjects compared to subjects with liver disease. In case of liver cirrhosis the observed relationship between bilirubin and ICG parameters is difficult to interpret. It is possible that the changes in ICG-elimination result from the disease itself and the observed changes in plasma bilirubin are simply a consequence of the liver disease without any effect on ICG uptake. Under the model assumption that bilirubin has a competitive inhibitory effect on ICG uptake the dependency of ICG parameters on bilirubin could be reproduced. In rat a clear effect of bilirubin plasma concentration (varied via injection) could be observed on ICG uptake, which supports our assumption (Paumgartner et al., 1969). Human data without liver disease but substantially altered bilirubin levels would be required to test the hypothesis that bilirubin is a competitive inhibitor of ICG uptake in humans.

Our study underlines the importance of quantifying and reporting factors affecting the inter-individual variability in liver function tests. The presented results have important implications for clinical testing of liver function with ICG as well as clinical studies involving ICG parameters. Most importantly, factors affecting ICG elimination must be quantified and reported alongside ICG parameters. Most of these factors can be easily determined in clinical practice such as body weight, sex, age in the anamnesis, plasma bilirubin via blood chemistry, hepatic blood flow and cardiac output via Doppler ultrasound, liver volume via imaging, and severity of cirrhosis using the CTP or MELD classification. The only factor difficult to obtain is the amount of OATP1B3 which would require invasive liver biopsy followed by protein quantification via immunohistochemistry. This could be a feasible approach in settings where liver biopsies are readily available, e.g., in hepatectomies. Clinical studies evaluating ICG elimination in different subgroups must account for differences in confounding factors such as age between groups. Especially in study designs comparing healthy controls (often young) with subjects with disease (often old) this is difficult to achieve. Our results provide quantitative information on the expected effect sizes.

In summary, the model shows a great potential in predicting the variability in ICG elimination in healthy as well as in cirrhotic subjects. By including variations in hepatic blood flow, hepatic transport proteins, liver volume, and body weight in the model simulation, new insights were gained on the correlation between ICG parameters and the dependency of the extraction ratio on hepatic blood flow. Important future questions are (i) how the information on underlying causes of inter-individual variability can be used

410 for an improved evaluation of ICG based liver function tests; and (ii) how this variability influences risk
411 assessment of postoperative survival after liver surgery based on ICG, e.g. the prediction of survival after
412 partial hepatectomy as proposed in (Köller et al., 2021).

CONFLICT OF INTEREST STATEMENT

413 All authors declare that the research was conducted in the absence of any commercial or financial
414 relationships that could be construed as a potential conflict of interest.

AUTHOR CONTRIBUTIONS

415 AK and MK designed the study, developed the computational model, implemented and performed the
416 analysis, and wrote the initial draft of the manuscript. JG provided support with PK-DB and data curation.
417 All authors discussed the results. All authors contributed to and revised the manuscript critically.

FUNDING

418 MK, AK and JG were supported by the Federal Ministry of Education and Research (BMBF, Germany)
419 within the research network Systems Medicine of the Liver (LiSyM, grant number 031L0054). MK and
420 AK were supported by the German Research Foundation (DFG) within the Research Unit Programme FOR
421 5151 "QuaLiPerF (Quantifying Liver Perfusion-Function Relationship in Complex Resection - A Systems
422 Medicine Approach)" by grant number 436883643.

DATA AVAILABILITY STATEMENT

423 All clinical data of ICG pharmacokinetics that was used in this work can be found in PK-DB available
424 from <https://pk-db.com>.

REFERENCES

- 425 Anzai, K., Tsuruya, K., Morimachi, M., Arase, Y., Hirose, S., Hirabayashi, K., et al. (2020). The impact of
426 a heterozygous SLCO1B3 null variant on the indocyanine green retention test. *Journal of pharmaceutical
427 sciences* 109, 3206–3209. doi:10.1016/j.xphs.2020.06.020
- 428 Berk, P. D., Potter, B. J., and Stremmel, W. (1987). Role of plasma membrane ligand-binding proteins in
429 the hepatocellular uptake of albumin-bound organic anions. *Hepatology (Baltimore, Md.)* 7, 165–176.
430 doi:10.1002/hep.1840070131
- 431 Branch, R. A., James, J. A., and Read, A. E. (1976). The clearance of antipyrine and indocyanine green in
432 normal subjects and in patients with chronic liver disease. *Clinical pharmacology and therapeutics* 20,
433 81–89. doi:10.1002/cpt197620181
- 434 Burns, E., Triger, D. R., Tucker, G. T., and Bax, N. D. (1991). Indocyanine green elimination in patients
435 with liver disease and in normal subjects. *Clinical science (London, England : 1979)* 80, 155–160
- 436 Burt, H. J., Riedmaier, A. E., Harwood, M. D., Crewe, H. K., Gill, K. L., and Neuhoff, S. (2016).
437 Abundance of hepatic transporters in caucasians: A meta-analysis. *Drug metabolism and disposition:
438 the biological fate of chemicals* 44, 1550–1561. doi:10.1124/dmd.116.071183
- 439 Caesar, J., Shaldon, S., Chiandussi, L., Guevara, L., and Sherlock, S. (1961). The use of indocyanine green
440 in the measurement of hepatic blood flow and as a test of hepatic function. *Clinical science* 21, 43–57
- 441 Cherrick, G. R., Stein, S. W., Leevy, C. M., and Davidson, C. S. (1960). Indocyanine green: observations
442 on its physical properties, plasma decay, and hepatic extraction. *The Journal of clinical investigation* 39,
443 592–600. doi:10.1172/JCI104072

- 444 de Graaf, W., Häusler, S., Heger, M., van Ginhoven, T. M., van Cappellen, G., Bennink, R. J., et al. (2011).
445 Transporters involved in the hepatic uptake of (99m)tc-mebrofenin and indocyanine green. *Journal of*
446 *hepatology* 54, 738–745. doi:10.1016/j.jhep.2010.07.047
- 447 D’Onofrio, M., De Robertis, R., Ruzzenente, A., Mantovani, W., Puntel, G., Crosara, S., et al. (2014).
448 Time-to-peak values can estimate hepatic functional reserve in patients undergoing surgical resection: a
449 comparison between perfusion ct and indocyanine green retention test. *Journal of computer assisted*
450 *tomography* 38, 733–741. doi:10.1097/RCT.0000000000000102
- 451 Fevery, J. (2008). Bilirubin in clinical practice: a review. *Liver international : official journal of the*
452 *International Association for the Study of the Liver* 28, 592–605. doi:10.1111/j.1478-3231.2008.01716.x
- 453 Fretzayas, A., Moustaki, M., Liapi, O., and Karpathios, T. (2012). Gilbert syndrome. *European journal of*
454 *pediatrics* 171, 11–15. doi:10.1007/s00431-011-1641-0
- 455 Gadano, A., Hadengue, A., Vachiry, F., Moreau, R., Sogni, P., Soupison, T., et al. (1997). Relationship
456 between hepatic blood flow, liver tests, haemodynamic values and clinical characteristics in patients
457 with chronic liver disease. *Journal of gastroenterology and hepatology* 12, 167–171. doi:10.1111/j.
458 1440-1746.1997.tb00401.x
- 459 Giacomini, K. M., Huang, S.-M., Tweedie, D. J., Benet, L. Z., Brouwer, K. L. R., Chu, X., et al.
460 (2010). Membrane transporters in drug development. *Nature reviews. Drug discovery* 9, 215–236.
461 doi:10.1038/nrd3028
- 462 Grainger, S. L., Keeling, P. W., Brown, I. M., Marigold, J. H., and Thompson, R. P. (1983). Clearance and
463 non-invasive determination of the hepatic extraction of indocyanine green in baboons and man. *Clinical*
464 *science (London, England : 1979)* 64, 207–212
- 465 Grundmann, U., Ziehmer, M., Raahimi, H., Altmayer, P., Larsen, R., and Büch, H. P. (1992). [effect of the
466 volatile anesthetics halothane, enflurane and isoflurane on liver circulation in the human]. *Anasthesiologie,*
467 *Intensivmedizin, Notfallmedizin, Schmerztherapie : AINS* 27, 406–413. doi:10.1055/s-2007-1000324
- 468 Haimerl, M., Schlabeck, M., Verloh, N., Zeman, F., Fellner, C., Nickel, D., et al. (2016). Volume-assisted
469 estimation of liver function based on gd-eob-dtpa-enhanced mr relaxometry. *European radiology* 26,
470 1125–1133. doi:10.1007/s00330-015-3919-5
- 471 Hashimoto, M. and Watanabe, G. (2000). Hepatic parenchymal cell volume and the indocyanine green
472 tolerance test. *The Journal of surgical research* 92, 222–227. doi:10.1006/jsre.2000.5893
- 473 Hucka, M., Bergmann, F. T., Chaouiya, C., Dräger, A., Hoops, S., Keating, S. M., et al. (2019). The
474 systems biology markup language (sbml): Language specification for level 3 version 2 core release 2.
475 *Journal of Integrative Bioinformatics*
- 476 Huet, P. M. and Lelorier, J. (1980). Effects of smoking and chronic hepatitis b on lidocaine and indocyanine
477 green kinetics. *Clinical pharmacology and therapeutics* 28, 208–215
- 478 Huet, P. M. and Villeneuve, J. P. (1983). Determinants of drug disposition in patients with cirrhosis.
479 *Hepatology (Baltimore, Md.)* 3, 913–918. doi:10.1002/hep.1840030604
- 480 Iwakiri, Y. (2014). Pathophysiology of portal hypertension. *Clinics in liver disease* 18, 281–291.
481 doi:10.1016/j.cld.2013.12.001
- 482 Jost, G., Wahlländer, A., von Mandach, U., and Preisig, R. (1987). Overnight salivary caffeine clearance: a
483 liver function test suitable for routine use. *Hepatology (Baltimore, Md.)* 7, 338–344. doi:10.1002/hep.
484 1840070221
- 485 Kagawa, T., Adachi, Y., Hashimoto, N., Mitsui, H., Ohashi, T., Yoneda, M., et al. (2017). Loss of organic
486 anion transporting polypeptide 1b3 function causes marked delay in indocyanine green clearance without
487 any clinical symptoms. *Hepatology (Baltimore, Md.)* 65, 1065–1068. doi:10.1002/hep.28950

- 488 Kamisaka, K., Yatsuji, Y., Yamada, H., and Kameda, H. (1974). The binding of indocyanine green and
489 other organic anions to serum proteins in liver diseases. *Clinica chimica acta; international journal of*
490 *clinical chemistry* 53, 255–264. doi:10.1016/0009-8981(74)90107-7
- 491 Kanstrup, I. L. and Winkler, K. (1987). Indocyanine green plasma clearance as a measure of changes in
492 hepatic blood flow. *Clinical physiology (Oxford, England)* 7, 51–54
- 493 Kawasaki, S., Sugiyama, Y., Iga, T., Hanano, M., Beppu, T., Sugiura, M., et al. (1988). Hepatic clearances
494 of antipyrine, indocyanine green, and galactose in normal subjects and in patients with chronic liver
495 diseases. *Clinical pharmacology and therapeutics* 44, 217–224. doi:10.1038/clpt.1988.140
- 496 Kawasaki, T., Moriyasu, F., Kimura, T., Someda, H., Fukuda, Y., and Ozawa, K. (1991). Changes in
497 portal blood flow consequent to partial hepatectomy: Doppler estimation. *Radiology* 180, 373–377.
498 doi:10.1148/radiology.180.2.2068298
- 499 Keating, S. M., Waltemath, D., König, M., Zhang, F., Dräger, A., Chaouiya, C., et al. (2020). Sbml level 3:
500 an extensible format for the exchange and reuse of biological models. *Molecular systems biology* 16,
501 e9110. doi:10.15252/msb.20199110
- 502 Kim, I. H., Kisseleva, T., and Brenner, D. A. (2015). Aging and liver disease. *Current opinion in*
503 *gastroenterology* 31, 184–191. doi:10.1097/MOG.0000000000000176
- 504 Kimoto, E., Yoshida, K., Balogh, L. M., Bi, Y.-A., Maeda, K., El-Kattan, A., et al. (2012). Characterization
505 of organic anion transporting polypeptide (oatp) expression and its functional contribution to the uptake
506 of substrates in human hepatocytes. *Molecular pharmaceutics* 9, 3535–3542. doi:10.1021/mp300379q
- 507 Köller, A., Grzegorzewski, J., Tautenhahn, M., and König, M. (2021). Prediction of survival after
508 hepatectomy using a physiologically based pharmacokinetic model of indocyanine green liver function
509 tests doi:10.1101/2021.06.15.448411
- 510 [Dataset] König, M. (2021a). matthiaskoenig/sbmlsim: 0.1.14 - sbml simulation made easy. doi:10.5281/
511 zenodo.4569155
- 512 [Dataset] König, M. (2021b). matthiaskoenig/sbmlutils: 0.4.12 - python utilities for sbml. doi:10.5281/
513 zenodo.4595467
- 514 [Dataset] König, M. and Rodriguez, N. (2019). matthiaskoenig/cy3sbml: cy3sbml-v0.3.0 - SBML for
515 Cytoscape. doi:10.5281/zenodo.3451319
- 516 Leevy, C. M., Mendenhall, C. L., Lesko, W., and Howard, M. M. (1962). Estimation of hepatic blood flow
517 with indocyanine green. *The Journal of clinical investigation* 41, 1169–1179. doi:10.1172/JCI104570
- 518 Leevy, C. M., Smith, F., Longueville, J., Paumgartner, G., and Howard, M. M. (1967). Indocyanine green
519 clearance as a test for hepatic function. evaluation by dichromatic ear densitometry. *JAMA* 200, 236–240
- 520 Martin, J. F., Mikulecky, M., Blaschke, T. F., Waggoner, J. G., Vergalla, J., and Berk, P. D. (1975).
521 Differences between the plasma indocyanine green disappearance rates of normal men and women.
522 *Proceedings of the Society for Experimental Biology and Medicine. Society for Experimental Biology*
523 *and Medicine (New York, N.Y.)* 150, 612–617
- 524 Maruhashi, T., Kihara, Y., and Higashi, Y. (2019). Bilirubin and endothelial function. *Journal of*
525 *atherosclerosis and thrombosis* 26, 688–696. doi:10.5551/jat.RV17035
- 526 Masuoka, S., Nasu, K., Takahashi, H., Kitao, A., Sakai, M., Ishiguro, T., et al. (2020). Impaired lesion
527 detectability on gadoteric acid-enhanced mr imaging in indocyanine green excretory defect: case series
528 of three patients. *Japanese journal of radiology* 38, 997–1003. doi:10.1007/s11604-020-00991-9
- 529 Møller, S., Hillingsø, J., Christensen, E., and Henriksen, J. H. (1998). Arterial hypoxaemia in cirrhosis:
530 fact or fiction? *Gut* 42, 868–874. doi:10.1136/gut.42.6.868
- 531 Møller, S., la Cour Sibbesen, E., Madsen, J. L., and Bendtsen, F. (2019). Indocyanine green retention
532 test in cirrhosis and portal hypertension: Accuracy and relation to severity of disease. *Journal of*

- 533 *gastroenterology and hepatology* 34, 1093–1099. doi:10.1111/jgh.14470
- 534 Namihisa, T., Nambu, M., Kobayashi, N., and Kuroda, H. (1981). Nine cases with marked retention
535 of indocyanine green test and normal sulfobromophthalein test without abnormal liver histology:
536 constitutional indocyanine green excretory defect. *Hepato-gastroenterology* 28, 6–12
- 537 NHANES (1999–2018). Centers for Disease Control and Prevention (CDC). National Center for Health
538 Statistics (NCHS). National Health and Nutrition Examination Survey Data. *Hyattsville, MD: U.S.
539 Department of Health and Human Services, Centers for Disease Control and Prevention*
- 540 Ott, P. (1998). Hepatic elimination of indocyanine green with special reference to distribution kinetics and
541 the influence of plasma protein binding. *Pharmacology & toxicology* 83 Suppl 2, 1–48
- 542 Paumgartner, G., Huber, J., and Grabner, G. (1969). Kinetics of hepatic dye absorption for indocyanine
543 green. influence of bilirubin and sodium glycocholate. *Experientia* 25, 1219–1223
- 544 Peng, K.-w., Bacon, J., Zheng, M., Guo, Y., and Wang, M. Z. (2015). Ethnic variability in the expression
545 of hepatic drug transporters: absolute quantification by an optimized targeted quantitative proteomic
546 approach. *Drug metabolism and disposition: the biological fate of chemicals* 43, 1045–1055. doi:10.
547 1124/dmd.115.063362
- 548 Pind, M.-L. L., Bendtsen, F., Kallemose, T., and Møller, S. (2016). Indocyanine green retention test (icg-r15)
549 as a noninvasive predictor of portal hypertension in patients with different severity of cirrhosis. *European
550 journal of gastroenterology & hepatology* 28, 948–954. doi:10.1097/MEG.0000000000000611
- 551 Prasad, B., Evers, R., Gupta, A., Hop, C. E. C. A., Salphati, L., Shukla, S., et al. (2014). Interindividual
552 variability in hepatic organic anion-transporting polypeptides and p-glycoprotein (abcb1) protein
553 expression: quantification by liquid chromatography tandem mass spectroscopy and influence of
554 genotype, age, and sex. *Drug metabolism and disposition: the biological fate of chemicals* 42, 78–88.
555 doi:10.1124/dmd.113.053819
- 556 Roberts, C. J., Jackson, L., Halliwell, M., and Branch, R. A. (1976). The relationship between liver volume,
557 antipyrine clearance and indocyanine green clearance before and after phenobarbitone administration in
558 man. *British journal of clinical pharmacology* 3, 907–913
- 559 Rowell, L. B., Blackmon, J. R., and Bruce, R. A. (1964). Indocyanine green clearance and estimated
560 hepatic blood flow during mild to maximal exercise in upright man. *The Journal of clinical investigation*
561 43, 1677–1690. doi:10.1172/JCI105043
- 562 Sakka, S. G. (2018). Assessment of liver perfusion and function by indocyanine green in the perioperative
563 setting and in critically ill patients. *Journal of clinical monitoring and computing* 32, 787–796. doi:10.
564 1007/s10877-017-0073-4
- 565 Sakka, S. G. and van Hout, N. (2006). Relation between indocyanine green (icg) plasma disappearance
566 rate and icg blood clearance in critically ill patients. *Intensive care medicine* 32, 766–769. doi:10.1007/
567 s00134-006-0109-6
- 568 Schipani, A., Egan, D., Dickinson, L., Davies, G., Boffito, M., Youle, M., et al. (2012). Estimation of the
569 effect of slco1b1 polymorphisms on lopinavir plasma concentration in hiv-infected adults. *Antiviral
570 therapy* 17, 861–868. doi:10.3851/IMP2095
- 571 Schmucker, D. L. (2005). Age-related changes in liver structure and function: Implications for disease ?
572 *Experimental gerontology* 40, 650–659. doi:10.1016/j.exger.2005.06.009
- 573 Schneck, D. W., Birmingham, B. K., Zalikowski, J. A., Mitchell, P. D., Wang, Y., Martin, P. D., et al.
574 (2004). The effect of gemfibrozil on the pharmacokinetics of rosuvastatin. *Clinical pharmacology and
575 therapeutics* 75, 455–463. doi:10.1016/j.clpt.2003.12.014
- 576 Shinohara, H., Tanaka, A., Kitai, T., Yanabu, N., Inomoto, T., Satoh, S., et al. (1996). Direct measurement
577 of hepatic indocyanine green clearance with near-infrared spectroscopy: separate evaluation of uptake

- 578 and removal. *Hepatology (Baltimore, Md.)* 23, 137–144. doi:10.1053/jhep.1996.v23.pm0008550033
579 Skak, C. and Keiding, S. (1987). Methodological problems in the use of indocyanine green to estimate
580 hepatic blood flow and icg clearance in man. *Liver* 7, 155–162. doi:10.1111/j.1600-0676.1987.tb00336.x
581 Somogyi, E. T., Bouteiller, J.-M., Glazier, J. A., König, M., Medley, J. K., Swat, M. H., et al. (2015).
582 libroadrunner: a high performance sbml simulation and analysis library. *Bioinformatics* 31, 3315–3321
583 Sullivan, J. I. and Rockey, D. C. (2017). Diagnosis and evaluation of hyperbilirubinemia. *Current opinion
584 in gastroenterology* 33, 164–170. doi:10.1097/MOG.0000000000000354
585 Vauthhey, J.-N., Abdalla, E. K., Doherty, D. A., Gertsch, P., Fenstermacher, M. J., Loyer, E. M., et al. (2002).
586 Body surface area and body weight predict total liver volume in western adults. *Liver transplantation :
587 official publication of the American Association for the Study of Liver Diseases and the International
588 Liver Transplantation Society* 8, 233–240. doi:10.1053/jlts.2002.31654
589 Wheeler, H. O., Cranston, W. I., and Meltzer, J. I. (1958). Hepatic uptake and biliary excretion of
590 indocyanine green in the dog. *Proceedings of the Society for Experimental Biology and Medicine.
591 Society for Experimental Biology and Medicine (New York, N.Y.)* 99, 11–14
592 Wood, A. J., Vestal, R. E., Wilkinson, G. R., Branch, R. A., and Shand, D. G. (1979). Effect of aging
593 and cigarette smoking on antipyrine and indocyanine green elimination. *Clinical pharmacology and
594 therapeutics* 26, 16–20
595 Wynne, H. A., Cope, L. H., Mutch, E., Rawlins, M. D., Woodhouse, K. W., and James, O. F. (1989). The
596 effect of age upon liver volume and apparent liver blood flow in healthy man. *Hepatology (Baltimore,
597 Md.)* 9, 297–301. doi:10.1002/hep.1840090222

Table 1. Overview of curated clinical studies.

Reference	PK-DB	PMID	ICG/Sampling	Protocol	Description
Anzai et al. (2020)	PKDB00501	32593714	ICG	Bolus: 0.5 mg/kg	The impact of a heterozygous SLCO1B3 null variant on the ICG retention test.
Branch et al. (1976)	PKDB00387	1277728	ICG	Bolus: 0.5 mg/kg	Clearance of ICG in healthy subjects and chronic liver disease (cirrhosis, hepatitis).
Burns et al. (1991)	PKDB00388	1848168	ICG	Bolus: 0.5 mg/kg; Infusion: 0.25 mg/min	ICG pharmacokinetics in healthy subjects and patients with liver disease.
Caesar et al. (1961)	PKDB00389	13689739	ICG	Bolus: 0.5 mg/kg; Infusion: 0.5 mg/min	Measuring hepatic blood flow and assessing hepatic function by ICG pharmacokinetics.
Cherrick et al. (1960)	PKDB00390	13809697	ICG	Bolus: 0.5 mg/kg	ICG pharmacokinetics in healthy subjects and patients with liver disease.
D'Onofrio et al. (2014)	PKDB00392	24834884	ICG	Bolus: 0.5 mg/kg	Comparison between perfusion CT and ICG-R15/ICG-PDR as an estimation of liver functional reserve for patients undergoing hepatectomy.
Gadano et al. (1997)	PKDB00394	9083919	ICG	Infusion: 0.4 mg/min (controls); 0.8 mg/min (cirrhotics). Priming dose (24 mg controls; 12 mg cirrhotics).	ICG-clearance and extraction ratio and their dependency on hepatic bloodflow in healthy subjects and in patients with hepatic fibrosis and cirrhosis.
Grundmann et al. (1992)	PKDB00396	1482735	ICG	Bolus: 0.3 mg/kg	Effect of anesthetics on ICG-pharmacokinetics and hepatic blood flow.
Haimerl et al. (2016)	PKDB00502	26186960	ICG	Bolus: 0.5 mg/kg	ICG-elimination in different severity of cirrhosis.
Hashimoto and Watanabe (2000)	PKDB00503	10896825	ICG	Bolus: 0.5 mg/kg	Correlation between body weight and liver volume and ICG-elimination.
Huet and Lelorier (1980)	PKDB00398	7398188	ICG	Bolus: 0.5 mg/kg	Effect of smoking and hepatitis B on ICG pharmacokinetics with estimates of hepatic blood flow.
Huet and Villeneuve (1983)	PKDB00399	6629320	ICG	Bolus: 0.5 mg/kg	ICG-pharmacokinetics in cirrhosis and chronic hepatitis with measurements of hepatic blood flow.
Jost et al. (1987)	PKDB00463	3557314	ICG	Bolus: 0.5 mg/kg	Salivary caffeine clearance as liver function tests.
Kagawa et al. (2017)	PKDB00504	27863442	ICG	Bolus: Dose not reported	Effect of loss of OATP1B3 on ICG-elimination.
Kanstrup and Winkler (1987)	PKDB00400	3816112	ICG	Infusion: 0.2 mg/min	Blood flow dependency of ICG-clearance.
Kawasaki et al. (1988)	PKDB00401	3396264	ICG	Bolus: 0.5 mg/kg	ICG-clearance in healthy subjects and patients with liver fibrosis and cirrhosis.
Leevy et al. (1962)	PKDB00404	14463639	ICG	Infusion: 0.3 and 1.5 mg/min/m ² with priming dose (10 mg).	Estimation of hepatic blood flow using ICG.
Leevy et al. (1967)	PKDB00405	6071462	ICG	Bolus: 0.5 mg/kg and 5.0 mg/kg	Estimation of liver function with ICG. Dose dependency of ICG-PDR.
Møller et al. (1998)	PKDB00409	9691928	ICG	Infusion: Rate not reported	Arterial hypoxaemia in cirrhosis. Correlation between ICG-clearance and CTP-score.
Møller et al. (2019)	PKDB00410	30221390	ICG	Infusion: 0.2 mg/min with priming dose (2mg)	Correlation between ICG-pharmacokinetics and CTP-score.
Pind et al. (2016)	PKDB00505	27172450	ICG	Infusion: 0.2 mg/min with priming dose	ICG-R15 as a noninvasive predictor of portal hypertension in patients with different severity of cirrhosis.
Roberts et al. (1976)	PKDB00425	973986	ICG	Bolus: 0.5 mg/kg	Dependency of ICG-clearance on liver volume.
Sakka and van Hout (2006)	PKDB00413	16544120	ICG	Bolus: 0.5 mg/kg	Relation between ICG-PDR and ICG-clearance in patients with non-liver disease.
Skak and Keiding (1987)	PKDB00506	3613884	ICG	Bolus: 0.5 mg/kg	Relation between ICG-clearance and hepatic blood flow.
Wood et al. (1979)	PKDB00426	445957	ICG	Bolus: 0.5 mg/kg	Age-dependency of ICG-clearance in smoking and nonsmoking individuals.
Peng et al. (2015)	-	25926430	Sampling	-	Variability in transport protein amounts.
Wynne et al. (1989)	-	2643548	Sampling	-	Correlation between age, body weight, liver volume and hepatic blood flow.
NHANES (1999-2018)	-	-	Sampling	-	Large set of anthropometric data of healthy subjects.

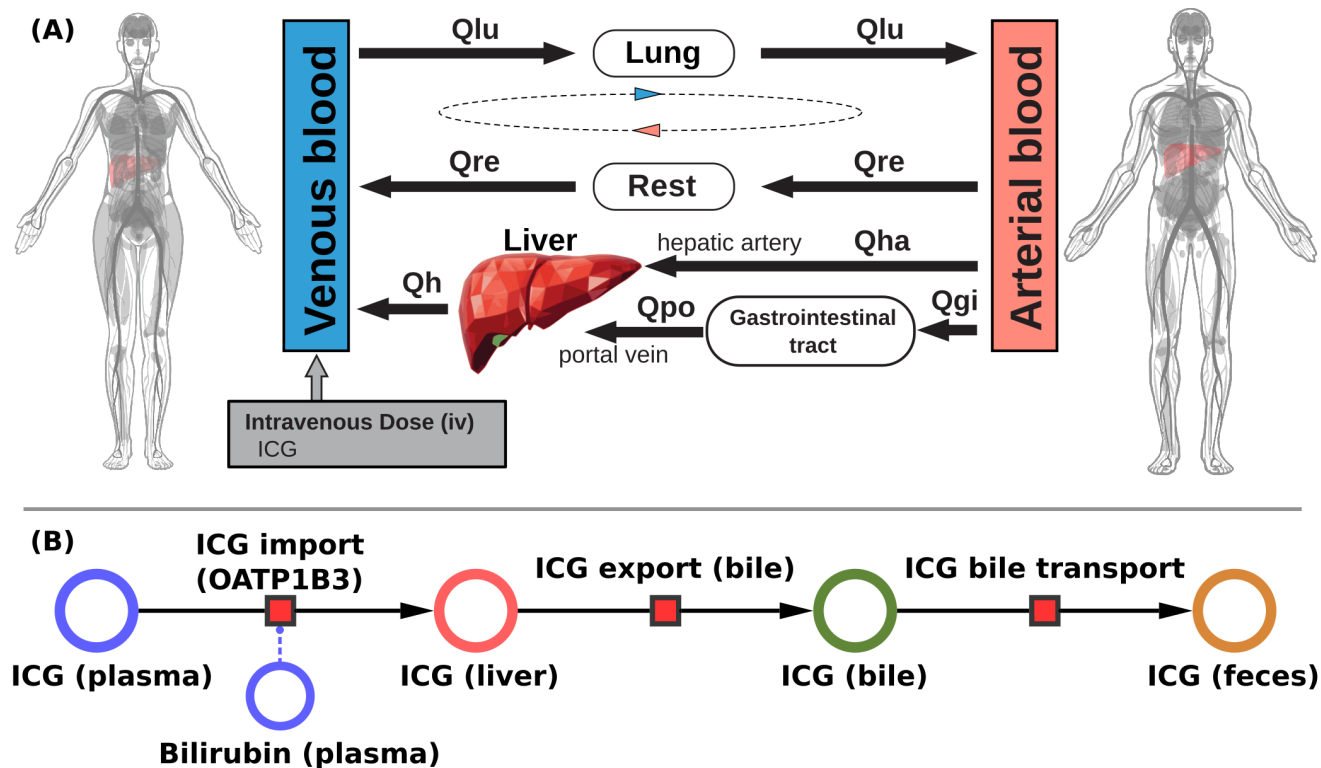


Figure 1. Model overview: **A:** PBPK model. The whole-body model for ICG consists of venous blood, arterial blood, lung, liver, gastrointestinal tract, and rest compartment (accounting for organs not modeled in detail). The systemic blood circulation connects these compartments. **B:** Liver model. ICG is taken up into the liver tissue (hepatocytes) via OATP1B3. The transport was modeled as competitively inhibited by plasma bilirubin. Hepatic ICG is excreted in the bile from where it is subsequently excreted in the feces. No metabolism of ICG occurs in the liver. Figure adapted from (Köller et al., 2021).

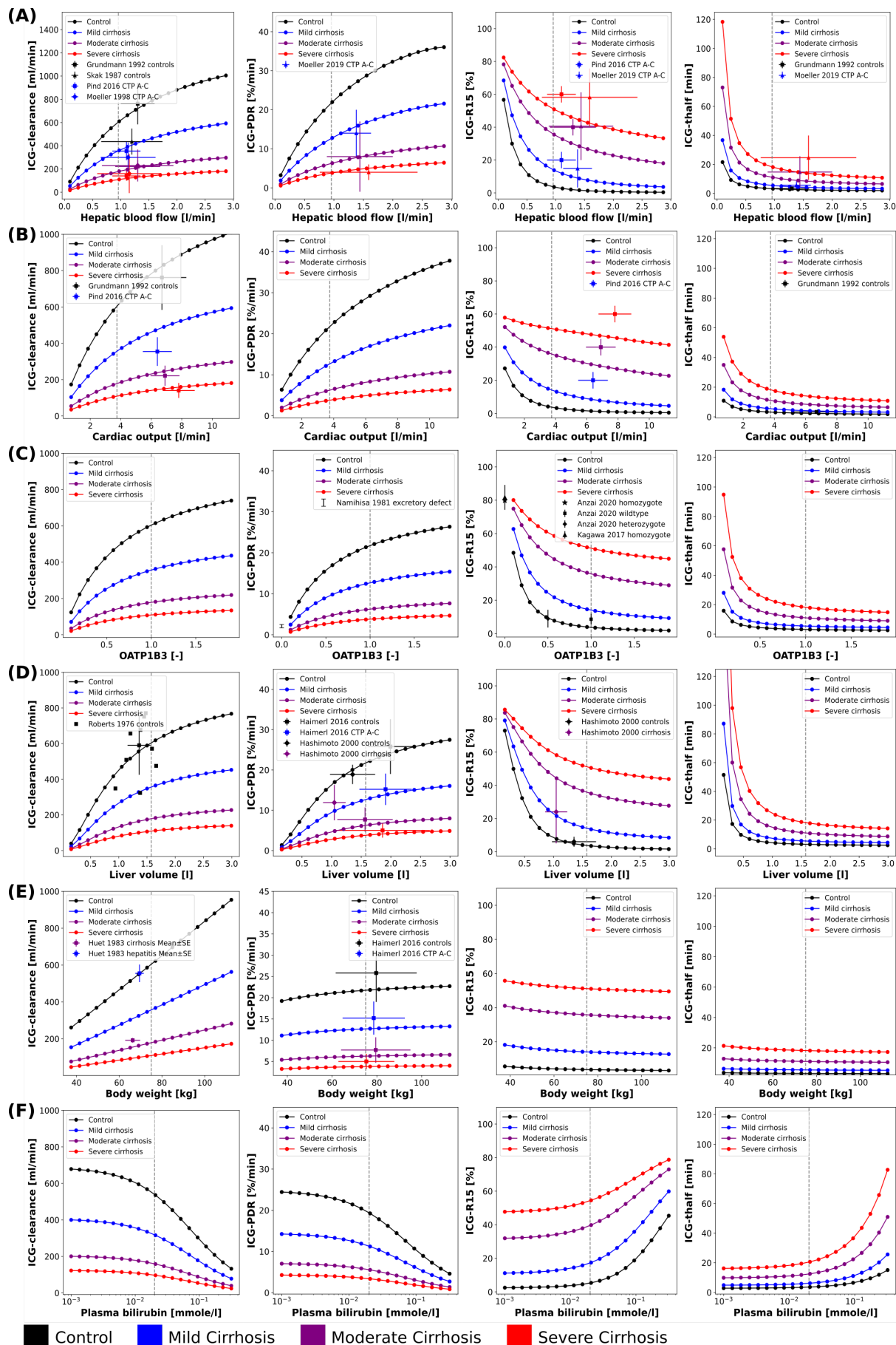


Figure 2. (Previous page) **Effect of physiological factors on ICG parameters:** The effect of hepatic blood flow, cardiac output, OATP1B3, liver volume, body weight, and plasma bilirubin on ICG-clearance, ICG-PDR, ICG-R15, and ICG-t_{1/2} were studied. Reference values of the model parameters, i.e. model parameters in the unchanged model, are indicated as vertical grey dashed lines. Black: control, blue: mild cirrhosis; purple: moderate cirrhosis, red: severe cirrhosis. **A:** Dependency on hepatic blood flow. Clinical data from Grundmann et al. (Grundmann et al., 1992), Pind et al. (Pind et al., 2016), Skak et al. (Skak and Keiding, 1987), and Moeller et al. (Møller et al., 1998, 2019). For additional data see Fig. 3. **B:** Dependency on cardiac output. Clinical data Grundmann et al. (Grundmann et al., 1992) and Pind et al. (Pind et al., 2016). **C:** Dependency on transport protein amount (OATP1B3). Clinical data from Anzai et al. (Anzai et al., 2020), Namihsa et al. (Namihsa et al., 1981), and Kagawa et al. (Kagawa et al., 2017). Heterozygote null variants with 0.5 activity, homozygote null variants with 0.0 activity. **D:** Dependency on liver volume. Clinical data from Haimerl et al. (Haimerl et al., 2016), Hashimoto et al. (Hashimoto and Watanabe, 2000), and Roberts et al. (Roberts et al., 1976). **E:** Dependency on body weight. Clinical data from Haimerl et al. (Haimerl et al., 2016) and Huet et al. (Huet and Villeneuve, 1983). **F:** Dependency on the plasma bilirubin concentration. For additional data see Fig. 4.

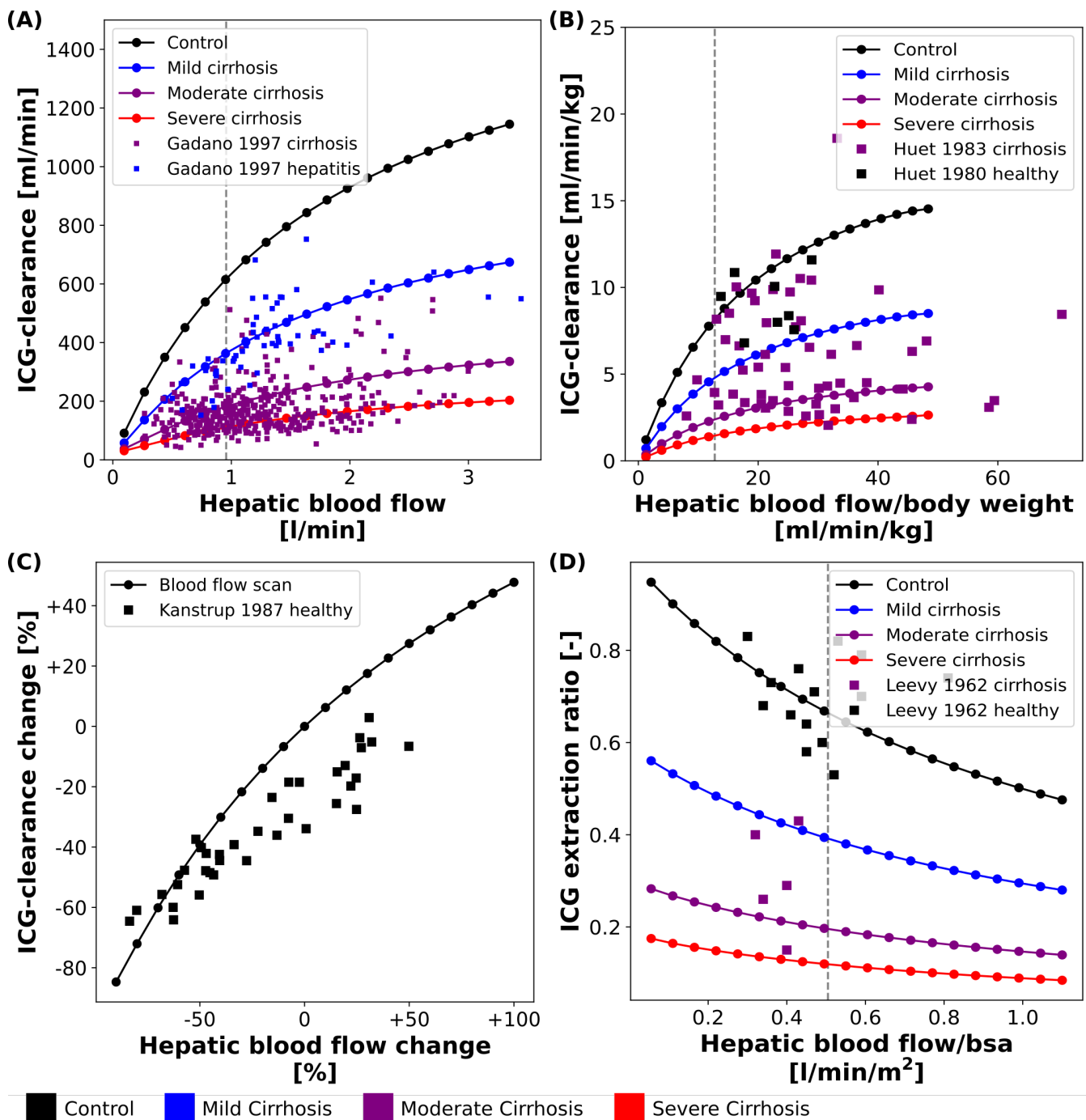


Figure 3. Effect of hepatic blood flow on ICG parameters: For model validation multiple blood flow experiments were simulated and compared to clinical data sets. Black: control, blue: mild cirrhosis; purple: moderate cirrhosis, red: severe cirrhosis. **A:** Dependency of ICG-clearance on hepatic blood flow. Clinical data of subjects with chronic hepatitis B and C and liver cirrhosis from Gadano et al. (Gadano et al., 1997). **B:** Dependency of ICG-clearance per kg body weight on hepatic blood flow per kg body weight. Clinical data of control and cirrhotic subjects from Huet et al. (Huet and Villeneuve, 1983; Huet and Lelorier, 1980). **C:** Dependency of ICG-clearance on externally changed hepatic blood flow. Clinical data of healthy subjects from Kanstrup and Winkler (Kanstrup and Winkler, 1987). **D:** Dependency of ICG extraction ratio on hepatic blood flow. Clinical data of control and cirrhotic subjects from Leevy et al. (Leevy et al., 1962).

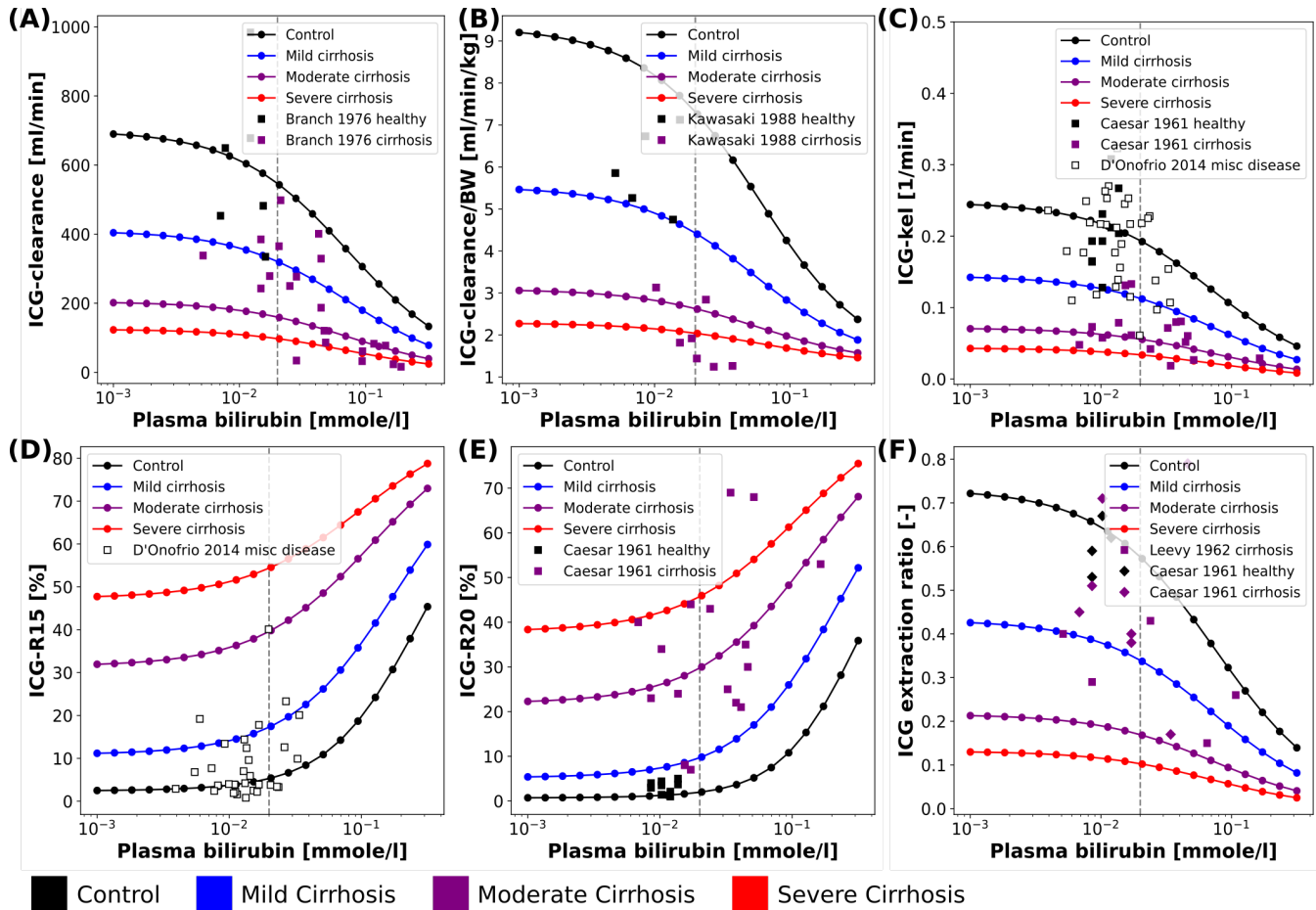


Figure 4. Effect of plasma bilirubin on ICG parameters: For model validation multiple plasma bilirubin experiments were simulated and compared to clinical data sets. Black: control, blue: mild cirrhosis; purple: moderate cirrhosis, red: severe cirrhosis. **A:** Dependency of ICG-clearance on the plasma bilirubin concentration. Clinical data of control and cirrhotic subjects from Branch et al. (Branch et al., 1976). **B:** Dependency of ICG-clearance per kg body weight on the plasma bilirubin concentration. Clinical data of control and cirrhotic subjects from Kawasaki et al. (Kawasaki et al., 1988). **C:** Dependency of ICG-kel on the plasma bilirubin concentration. Clinical data of control and cirrhotic subjects from Caesar et al. (Caesar et al., 1961). Clinical data of subjects with other liver diseases from D'Onofrio et al. (D'Onofrio et al., 2014). **D:** Dependency of ICG-R15 on the plasma bilirubin concentration. Clinical data of subjects with other liver diseases from D'Onofrio et al. (D'Onofrio et al., 2014). **E:** Dependency of ICG-R20 on the plasma bilirubin concentration. Clinical data of control and cirrhotic subjects from Caesar et al. (Caesar et al., 1961). **F:** Dependency of ICG extraction ratio on the plasma bilirubin concentration. Clinical data of control and cirrhotic subjects from Caesar et al. and Leevy et al. (Caesar et al., 1961; Leevy et al., 1962).

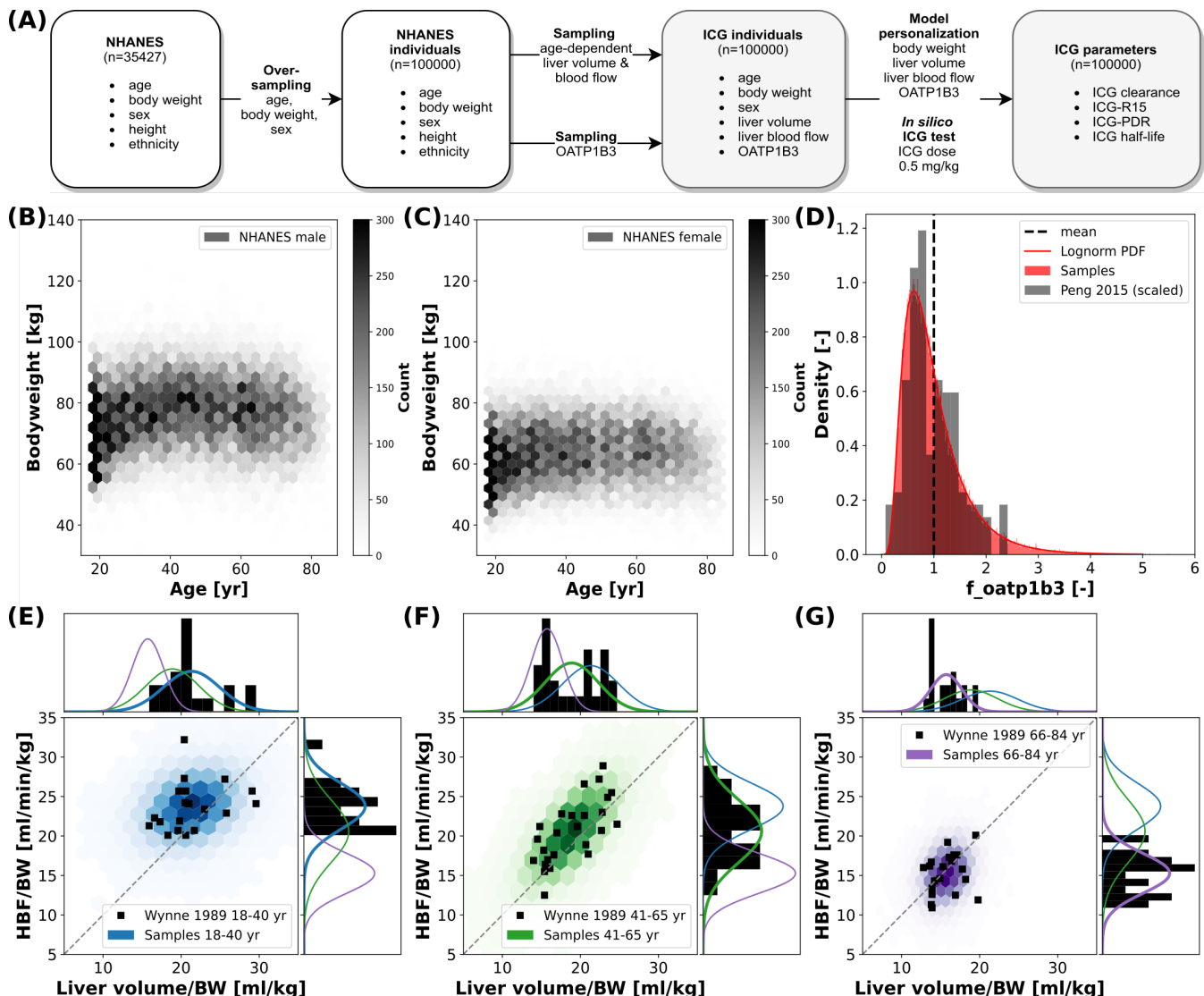


Figure 5. In silico population: ICG elimination was simulated for an *In silico* population consisting of n=100000 individuals (see Fig. 1E for workflow). Subjects are sampled from the NHANES cohort thereby accounting for the existing covariances between sex, age, body weight, height and ethnicity. **A:** Workflow to simulate ICG elimination in a large *In silico* population consisting of n=100000 individuals. **B, C:** Dependency of body weight on age in men and women. Data from NHANES (NHANES, 1999-2018) depicted as hexbin with shading corresponding to number of subjects (hexbins containing ≥ 300 subjects are encoded in black). **D:** Lognormal density distribution of OATP1B3 amount. Clinical data (grey) from Peng et al. (Peng et al., 2015) was normalized to the model parameter f_oatp1b3 describing the change in OATP1B3 amount relative to the model reference value. **E-G:** Distributions of hepatic blood flow per kg body weight and liver volume per kg body weight in 3 different age groups: blue - 18-40 yr; green - 41-65 yr; purple - 66-84 yr. Clinical data (black) from Wynne et al. (Wynne et al., 1989).

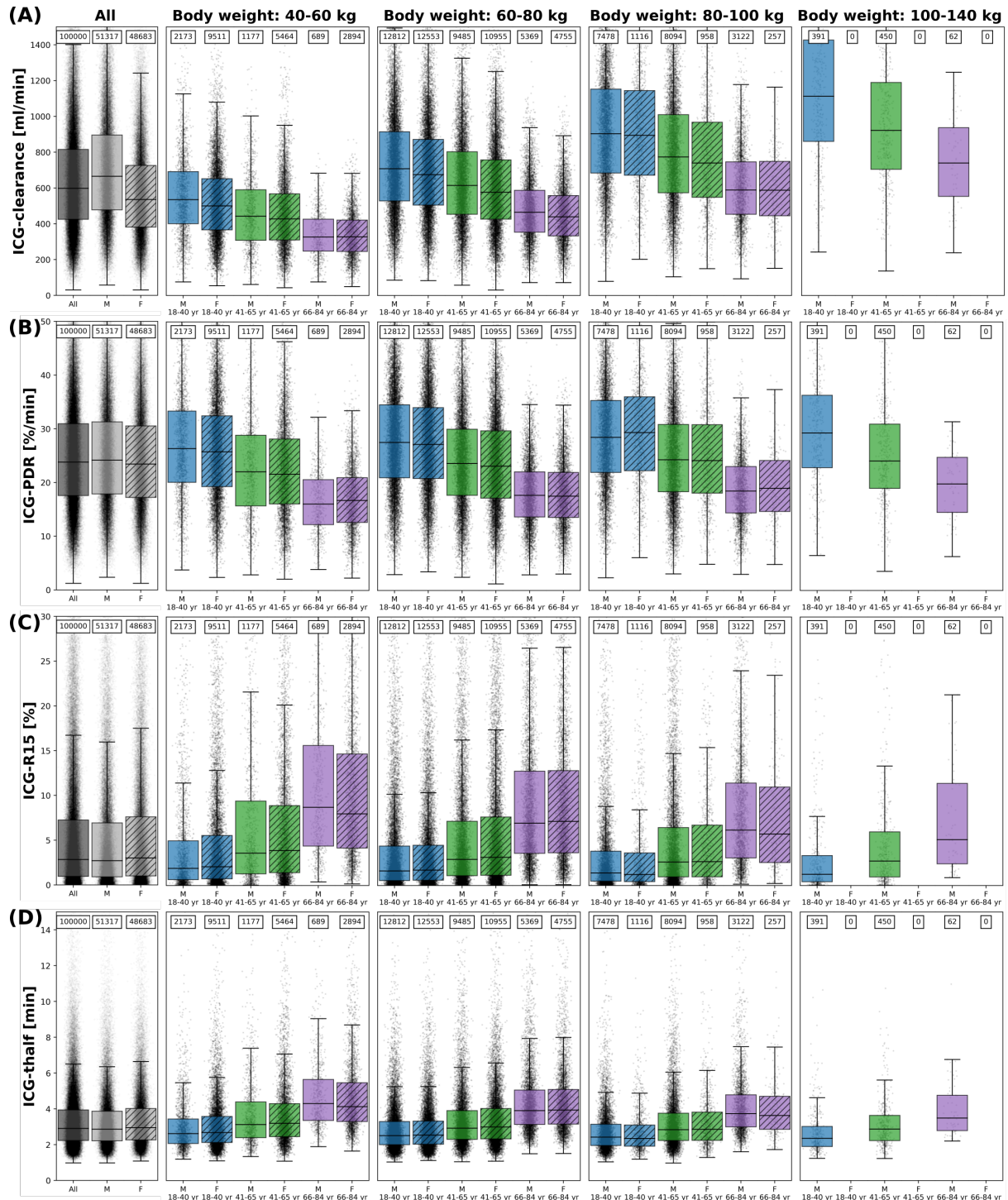


Figure 6. ICG parameters healthy *in silico* population: The dependency of **A** ICG-clearance [ml/min], **B** ICG-PDR [%/min], **C** ICG-R15[%], and **D** ICG-t_{1/2} [min] on body weight, sex and age in n=100000 individuals. Results are stratified by body weight class (40-60 kg, 60-80 kg, 80-100 kg, 100-140 kg), age group (blue - 18-40 yr; green - 41-65 yr; purple - 66-84 yr) and sex (M - unshaded; F - shaded). No women exist with body weight > 100 kg in the cohort. The sample size of the respective subgroups are depicted above each boxplot. The box extends from the lower to upper quartile values of the data, with a line at the median with whiskers as defined by Tukey. Individual data points are plotted for all subgroups. Subjects were simulated as healthy controls. For the corresponding results in mild cirrhosis, moderate cirrhosis, and severe cirrhosis see Supplementary Figure 1, 2 and 3, respectively.

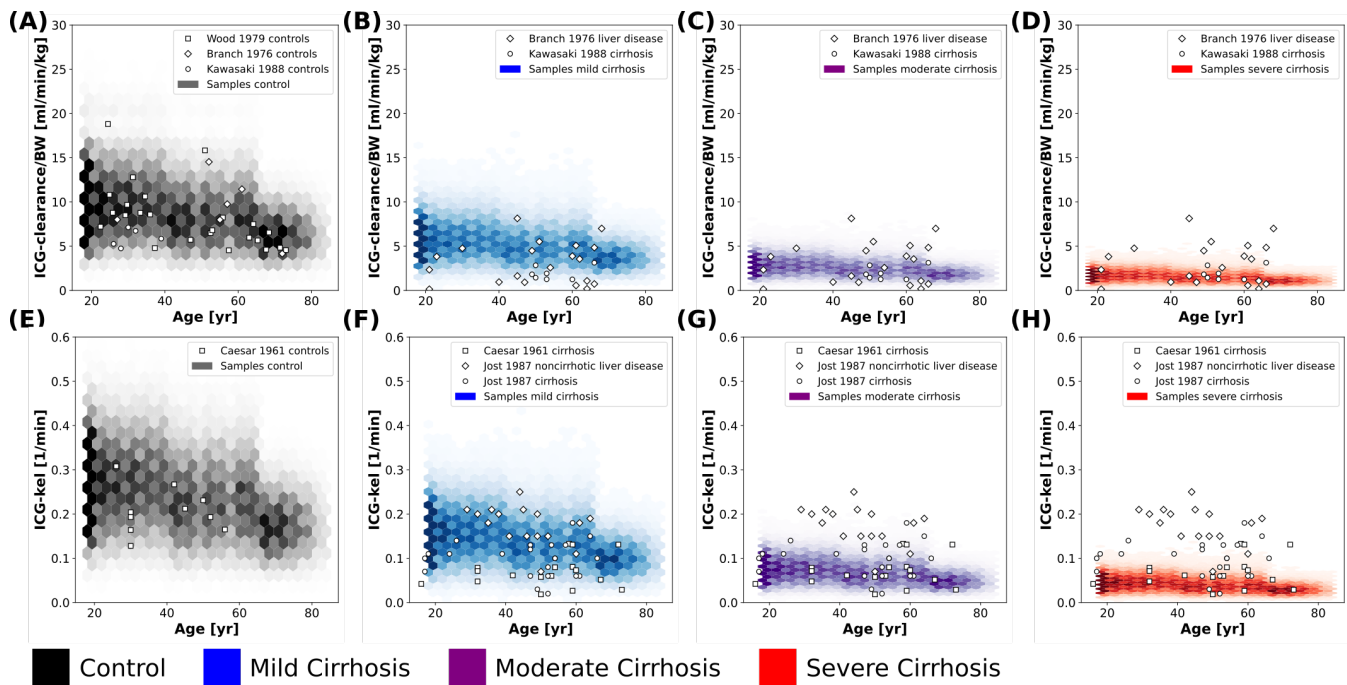


Figure 7. Validation of *in silico* population predictions: Age dependency of ICG clearance per body weight A-D and kel E-H in the population depicted as hexbins. Simulations were performed for healthy control (black), mild cirrhosis (blue), moderate cirrhosis (purple), and severe cirrhosis (red). Clinical data of controls from Wood et al., Branch et al., Kawasaki et al., and Caesar et al. (Wood et al., 1979; Branch et al., 1976; Kawasaki et al., 1988; Caesar et al., 1961) and cirrhotic subjects from Branch et al., Kawasaki et al., Caesar et al., and Jost et al. (Branch et al., 1976; Kawasaki et al., 1988; Caesar et al., 1961; Jost et al., 1987).

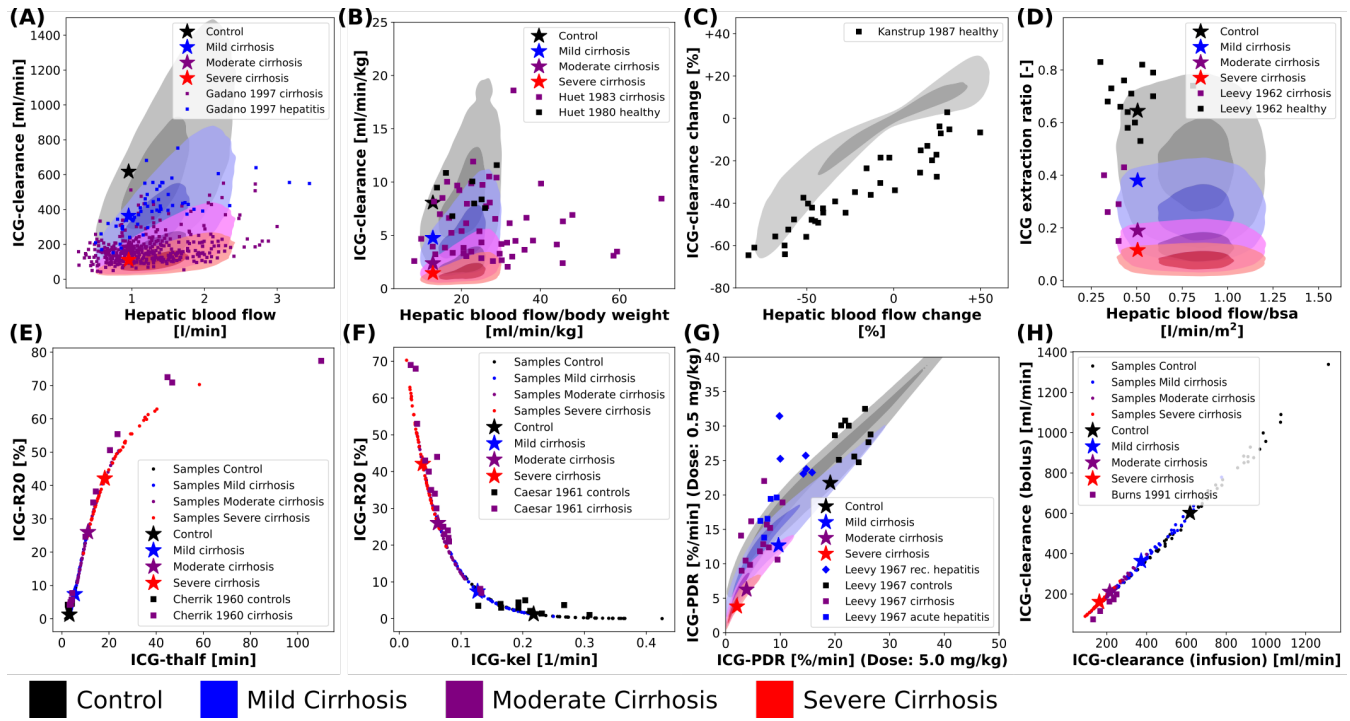


Figure 8. Variability analysis - model validation: The simulations were performed for four different cirrhosis degrees (except in C). Black: control, blue: mild cirrhosis; purple: moderate cirrhosis, red: severe cirrhosis. Stars depict the respective reference simulations. **A-D, G:** The identical simulations as in Fig. 3 were performed for the entire *in silico* population ($n=100000$). **E, F and H:** Simulations were performed for a subset of the *in silico* population ($n=50$). **E:** Correlation between ICG-R20 and ICG-t_{1/2}. Clinical data of control and cirrhotic subjects from Cherrick et al. (Cherrick et al., 1960). **F:** Correlation between ICG-R20 and ICG-kel. Clinical data of control and cirrhotic subjects from Caesar et al. (Caesar et al., 1961). **G:** Correlation between ICG-PDR after an ICG dose of 0.5 mg/kg and 5.0 mg/kg. Clinical data of control subjects and subjects with hepatitis (recovering and acute) and liver cirrhosis from Leevy et al. (Leevy et al., 1967). **H:** Correlation between ICG-clearance after a bolus administration and a constant infusion of ICG. Clinical data of cirrhotic subjects from Burns et al. (Burns et al., 1991)

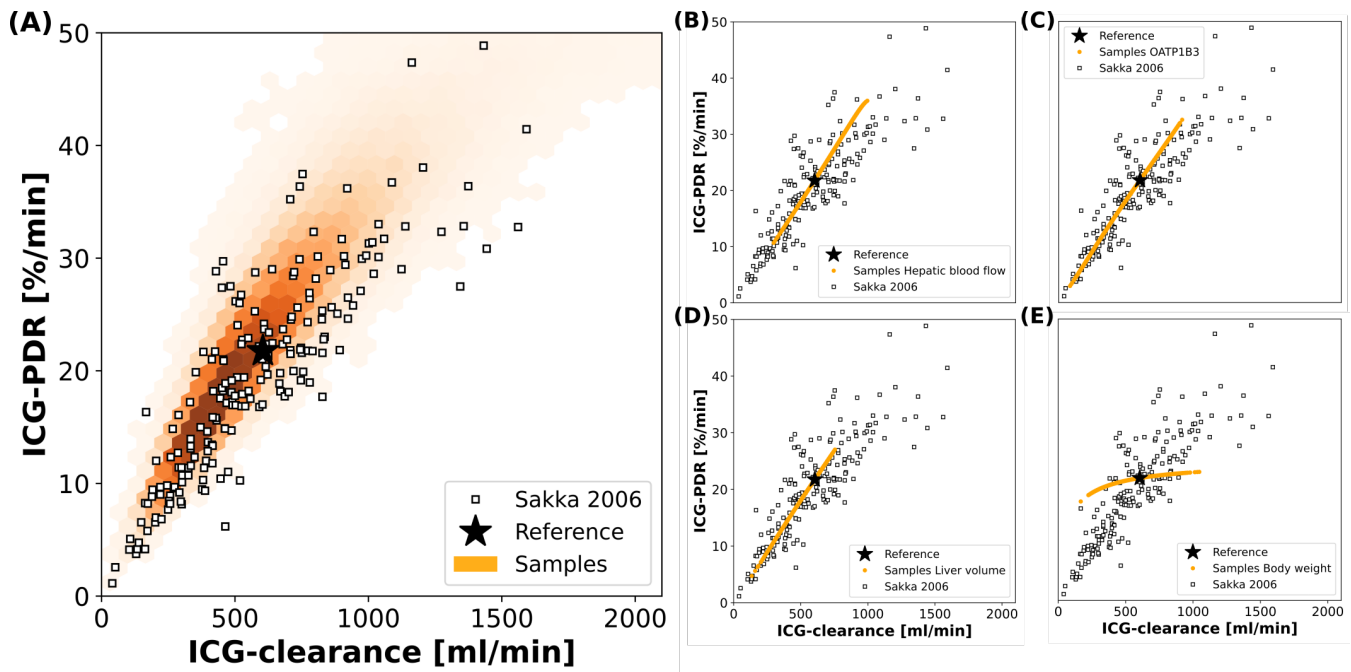


Figure 9. Contributions to population variability: Relationship between ICG-clearance and ICG-PDR with clinical data from Sakka and van Hout (Sakka and van Hout, 2006). **A:** Results of the simulations of the complete *in silico* population ($n=100000$). **B-E** Results of simulations, when hepatic blood flow, OATP1B3 level, liver volume, or body weight were varied individually in the range covered by the population. The respective other factors were set to their respective reference values in the simulation. Stars depict the reference simulation of the model.